A Versatile Mussel-Inspired Dynamic Biointerface: From Specific Cell Behavior Modulation to Selective Cell Isolation

Lei Liu,[a],* Xiaohua Tian,[a] Yue Ma,[b] Yuqing Duan,[c] Xin Zhao [d] and Guoqing Pan [a],*

[a]   Prof. Dr. L. Liu, X. Tian, Prof. Dr. G. Pan Institute for Advanced Materials, School of Materials Science and Engineering, Jiangsu University, Zhenjiang, Jiangsu, 212013, China. Email: liul@ujs.edu.cn (L. Liu); panguoqing@ujs.edu.cn (G. Pan)

[b]   Dr. Yue Ma. School of Chemistry and Chemical Engineering, Jiangsu University, Zhenjiang, Jiangsu, 212013, China

[c]   Prof. Dr. Y. Duan. School of Food and Biological Engineering, Jiangsu University, Zhenjiang, China

[d]   Dr. X. Zhao Department of Biomedical Engineering, The Hong Kong Polytechnic University, Hung Hom, Hong Kong, China

Abstract: We report a novel dynamic biointerface based on reversible catechol-boronate chemistry. We first biomimetically designed peptides with catechol-containing sequence and cell-binding sequence at each end. The peptides were then reversibly bound on a phenylboronic acid (PBA)-containing polymer-grafted substrate through sugar-responsive catechol-boronate interactions. The resultant biointerface is thus capable of dynamic presentation of the bioactivity (i.e., the cell-binding sequence) by virtue of changing sugar concentrations in the system (similar to human glycemic volatility). In addition, the sugar-responsive biointerface enables not only dynamic modulation of stem cell adhesion behaviors but also selective isolation of tumor cells. Considering the highly biomimetic nature and biological stimuli-responsiveness, this mussel-inspired dynamic biointerface thereby holds great promise in both fundamental cell biology research and advanced medical applications.

Dynamic receptor-ligand interactions between cells and the extracellular matrix (ECM) are crucial to cellular processes.[1] Changes in these interactions as a consequence of external or internal biological stimuli will lead to dynamic cell behaviors.[1b, 1c] As the most fundamental cell behavior, cell adhesion features the most conspicuous dynamic in bio-systems. For example, tissue repair involves a continual and mutual conversion between cell adhesion and migration in the wound site;[2] and cancer metastasis results from cell detachment from a solid tumor and resettlement of the detached tumor cells (circulating tumor cells, CTCs) along the blood vessel.[3] Undoubtedly, the reversible cell adhesion behaviors triggered by dynamic receptor-ligand interactions at the interface of the cell membrane and ECM, are closely related to both physiology and pathology.

As ECM mimics, synthetic biointerfaces that enable reversible presentation of bioactive ligands and subsequently modulation of cell adhesion behaviors has attracted extensive attention.[1c, 4] To this end, various cleavable or transformable chemical bonds that can respond to different types of stimuli, including temperature,[5] pH,[6] potential,[7] specific molecules,[8] UV or near-infrared light, [6, 9] have been successfully employed for dynamic immobilization of cell-binding ligands (e.g., adhesive peptides, proteins and DNA aptamers, etc.). These dynamic biointerfaces can be used for the control of cell adhesion and even selective cell capture and release, thus showing potentials in real-time cell biology, regenerative medicine and theranostics. [1c, 4b, 10]

Despite the vast prospects, current dynamic biointerfaces still have critical problems in practical applications. 1) External stimuli required in most of these systems are not biological stimuli and are probably invasive to living cells. 2) Current systems usually involve a release of the bioactive ligand complexes, in which the chemical linkers (e.g., synthetic chemicals or polymers) are non-biocompatible and potentially harmful to cells. 3) Their general applicability, from cell behavior modulation (i.e., fundamental cell biology experimentation) to selective cell isolation (i.e., cell-based tissue engineering and cancer diagnosis), is still in its infancy. Therefore, exploitation of new biointerfaces with responsiveness to biological stimuli, low- or non-toxic bioligand complexes, and a versatile performance that enables not only dynamic modulation of cell adhesion behaviors but also selective capture and release of targeted cells, is very challenging but highly anticipated.

Herein, we present a new dynamic biointerface based on mussel-inspired peptide mimics [11] and sugar-responsive reversible covalent bonds.[12] We first designed biomimetic peptides ((DOPA)$_4$-**Y-X**) that composed of a cell-binding sequence **X** at the C-terminus, a non-bioactive spacer sequence **Y**, and a tetrapeptide (DOPA)$_4$ with catechol groups at the N-terminal end (Scheme 1a). DOPA is a catecholic amino acid 3,4-dihydroxy-L-phenylalanine that is abundant in mussel secreted proteins (Scheme 1b). [13] The catechol group in DOPA can bind with phenylboronic acid (PBA) through the formation of dynamic catechol/PBA ester.[11b] Hence, the (DOPA)$_4$ in the
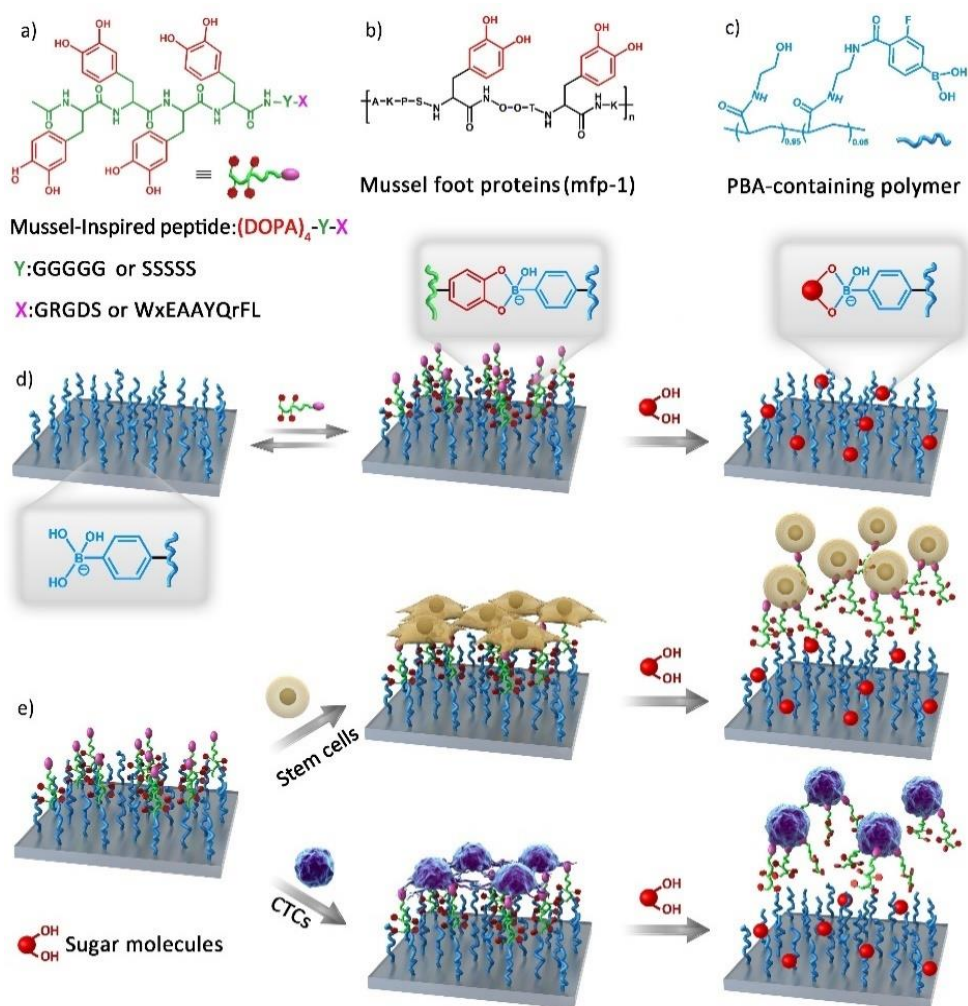
Scheme 1. a) Mussel-inspired peptides with catechol groups (DOPA) and bioactive motifs at the end. b) Natural mussel foot proteins (Mfp-1). c) Structural formula of the PBA-containing polymers on quartz slides. d) Sugar-responsiveness of the dynamic biointerface. e) Specific modulation of stem cell adhesion behaviors and selective isolation of tumor cells on the dynamic biointerfaces.

mussel-inspired peptides could act as a stable anchor onto a PBA-containing substrate, and leave the bioactive **X** sequence exposed for interaction with the cell-membrane receptor. Moreover, the addition of sugars with *cis*-diol groups (e.g., glucose or fructose) to the system could induce the release of surface bound peptides through molecular exchange of the catechol groups with PBA (Scheme 1c),[14] implying the potential to dynamically display bioactivity by a stimulus similar to human glycemic volatility.[15] Furthermore, we chose different cell binding sequences in the peptides and applied them for both the modulation of specific stem cell adhesion behaviors and the isolation of targeted tumor cells. We anticipate that the biomimetic nature of the peptides, the sugar-sensitive internal biological stimulus and the potential versatility in our system would facilitate the wide applications in cell biology and biomedicine.

As part of the dynamic biointerface, the PBA-containing substrate was prepared through photo-initiated polymerization of a hydrophilic monomer 2-hydroxyethyl acrylamide (HEAAm) and a sugar-responsive monomer 4-(2-acrylamidoethylcarbamoyl)-3-fluorophenylboronic acid (AFPBA) on a methacrylated quartz slide (Scheme 1d, left) (see details in Figure S1-S2 and the Supporting Information). The polymer-grafted quartz slides were then characterized by ellipsometry, Fourier-transform infrared spectroscopy (FT-IR), X-ray photoelectron spectroscopy (XPS), atomic force microscopy (AFM) and static contact angle experiments. Significant increases in the thickness (~ 5.7 nm in dry state), surface roughness, boron and fluorine content of the grafted substrates confirmed the successful grafting of poly(HEAAm-*co*-AFPBA) brushes (Figure S3-S5). Moreover, the polymer-grafted surface showed extremely high hydrophilicity (Figure S6). This peculiarity could be attributed to a large amount of HEAAm blocks in the polymers, and will be useful to reduce protein adsorption and nonspecific cell binding.[8e]

The biomimetic peptides were prepared by a standard Fmoc-based solid-phase peptide synthesis strategy. [11b, 11c] We first designed and synthesized a fluorescein isothiocyanate-labelled non-bioactive peptide FITC-(DOPA)$_4$-G$_5$-RGES to check the sugar-responsiveness of the damic biointerface (Figure S7). Peptide binding on the poly(HEAAm-*co*-AFPBA)-grafted surface was monitored by quartz crystal microbalance with dissipation monitoring (QCM-D) (Figure 1a and S8). Real time QCM-D frequency (*f*) of the PBA-contaning surface showed a sharp

decrease after addition of the peptide, indicating rapid peptide binding through PBA/catechol esterification. Upon the addition of sugar (e.g., glucose or fructose), the frequency showed a further decrease in 30s, followed by a slight increase (Figure 1a and S9). This phenomenon could correspond to the initial sugar binding with residual PBA groups and the later peptide release caused by molecular exchanging (Scheme 1d). [14] The peptide release process was further confirmed by monitoring the fluorescence intensity on the peptide-bound surface. As shown in Figure 1b and S9, the surface fluorescent intensity decreased dramatically after incubation in the sugar solution for 10 min, indicating a rapid peptide release. Considering the Δf value being proportional to the mass of bound molecules,[16] we estimated that ~70.5 % of the bound peptide could be released after incubation in fructose solution (60 mM) for 5 min (Figure 1a). In contrast, only 42.8 % of the peptide was released with the addition of glucose (Figure S8), due to the lower binding constant between glucose and PBA.[17] Nevertheless, these results confirmed that the PBA-containing surface could efficiently bind the mussel-inspired peptides and release them via sugar-responsive molecular exchanging, implying its potential for dynamic display of bioactivity in conditions involving biological stimulus.
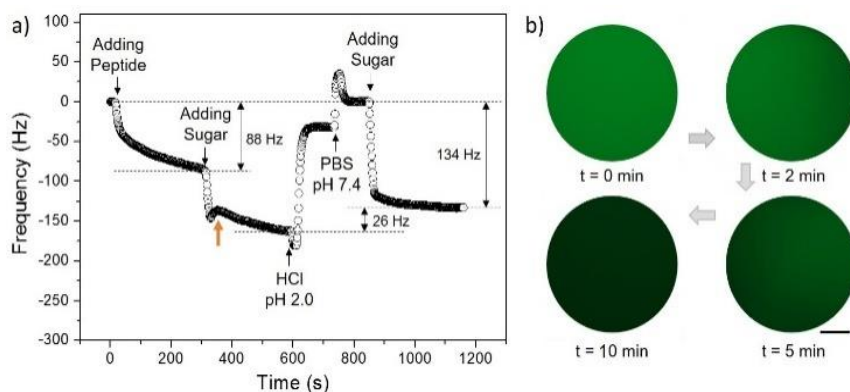

Figure 1. a) Real time QCM-D frequency shifts of the PBA-containing surface exposed to different solutions. The concentrations of FITC-(DOPA)$_4$-G$_5$-RGES and sugar (fructose) were 0.05 and 60.0 mM, respectively. b) Changes in fluorescent intensity on the FITC-peptide-bound substrate after incubation in PBS with 60 mM fructose. Scale bar is 1 mm.

Based on the dynamic property, we then checked its potential to modulate stem cell adhesion behaviors. To induce specific cell adhesion, the integrin-targeted peptide (RGD) was employed to design a new biomimetic peptide (DOPA)$_4$-S$_5$-GRGDS (Figure S10).[18] Human bone marrow-derived mesenchymal stem cells (BM-MSCs) were chosen as model cells due to their wide applications in cell-based tissue engineering and regenerative medicine. Without binding (DOPA)$_4$-S$_5$-GRGDS, cell morphology on the PBA-containing substrate only showed non-adhesive round shape after 3 hours culture in α-minimal essential medium (α-MEM) (Figure 2a). Such excellent cell-repellant properties were presumably due to the high hydrophilicity of poly(HEAAm-*co*-AFPBA) brushes (Figure S5), thus reducing nonspecific protein adsorption. In contrast, the cell adhesion behavior was dramatically improved following the introduction of (DOPA)$_4$-S$_5$-GRGDS. We observed typically adhered cells with a spreading shape on the RGD-bound surface (Figure 2a and S11). Another observation also worth noting is the poor cell adhesion property on the surface bound with non-adhesive RGE peptide (Figure S11), further confirming the specific cell adhesion mechanism triggered by RGD/integrin interactions. We subsequently applied 4′-6-diamidino-2-phenylindole (DAPI) and fluorescein phalloidin to stain the nuclei and F-actin of the adhered cells, respectively. The F-actin networks of cells on RGD-bound surface exhibited typical focal adhesion patterns and spreading shapes (inset in Figure 2a and S12).[19] However, only sporadic round cells with no stress fibers were found on the unbound surface. These results suggested that the dynamic biointerface with integrin-targeted RGD peptide could introduce specific cell adhesion.

In addition, sugar-triggered changes in cell adhesion behavior on the dynamic biointerface were also examined. After adding sugar into the medium (60 mM fructose), a gradual transition of the cell morphology from a spread-out shape to a round shape was clearly observed (Figure 2b and S13). After incubation at 37 °C for 20 min, all the adhered cells showed a dramatical change in adhesion status, where more than 90% of the cells were easily removable after mild rinsing. This phenomenon is due to the sugar-induced release of (DOPA)$_4$-S$_5$-GRGDS, resulting in the disappearance of cell adhesive forces and subsequently cell detachment. We further found that the detached cells could re-adhere after changing the medium with new α-MEM and feeding the system with (DOPA)$_4$-S$_5$-GRGDS (Figure S14). In contrast, the adhered cells on tissue culture polystyrenes plates showed no change in the adhesion status after sugar treatment (Figure S15). Altogether, these results demonstrated that our system with a reversible RGD peptide presentation could be employed to modulate the behaviors of stem cell adhesion. More importantly, after re-adhesion onto a new petri dish, the detached cells exhibited excellent cell viability equivalent to the cells without sugar treatment (Figure S16). This finding further indicated that sugar-regulated cell behavior on our dynamic biointerface occurred in a non-invasive manner, thus holding promise in stem cell-based regenerative medicine.

Another potential of this dynamic biointerface is in selective cell capture and release, which has shown to be promising in cell-based disease diagnosis (e.g., CTCs isolation).[20] As proof of concept, we designed another peptide (DOPA)$_4$-S$_5$-WxEAAYQrFL for targeting tumor cells (Figure S17). The sequence WxEAAYQrFL is a proteolytically stable breast cancer-targeting peptide derived from a 12-mer peptide p160 identified by using *in vivo* phage display for cancer targeting (e.g., MCF-7, a human mammary adenocarcinoma cell line).[21] Given this, the cancer-targeting peptide (DOPA)$_4$-S$_5$-WxEAAYQrFL was bound onto the PBA-containing surface to demonstrate the ability to selectively isolate MCF-7 cells. The WxEAAYQrFL-bound surface was incubated in RPMI 1640 medium suspending with MCF-7 cells and the bare surface was used as a control. After incubation for 60 min, an abundance of MCF-7 cells were captured onto the WxEAAYQrFL-bound surface with a spreading cell morphology (Figure S18) and the surface captured cell density was 8460 ± 830 cm^{-2} (Figure 3a). In contrast, the bare surface (control) showed almost no bound cells. Nevertheless, when we added (DOPA)$_4$-S$_5$-WxEAAYQrFL into the control system, the surface exhibited significantly increased MCF-7 cell capture capacity (Figure S19). It was also found that the peptide-bound surface showed a time-dependent cell-capture property (Figure S20). The maximum cell-capture capacity could reach up to 11320 ± 490 cm^{-2} in 90 min. This capacity is comparable to a previously reported nanostructured surface immobilized with a cell-targeting antibody.[5a] We then incubated the cell-bound slides into a medium with 60 mM fructose to examine its cell release property. As shown in Figure 3b and S21, the surface generated an efficient release of the captured MCF-7 cells. After incubating for 30 min, ~ 99% of the MCF-7 cell was released, demonstrating a high cell-release efficiency. Furthermore, the dynamic biointerface was applicable for 3 cycles of capture/release assays (Figure S22), indicating its excellent reusability for tumor cell capture and release.
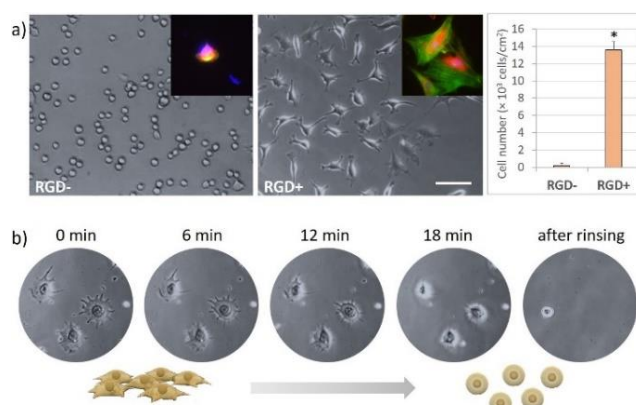

Figure 2. a) Representative micrographs of BM-MSCs after culture for 3 hours on the surfaces without (RGD-) or with (DOPA)$_4$-S$_5$-GRGDS (RGD+). The cell-adhesion efficiency was quantified in the right histogram. Insets are representative fluorescence images of adhered cells. Statistically significant differences are indicated by * $p<0.001$ as compared with others. Scale bar is 100 μm. b) Time-dependent changes of cell morphology on the RGD-bound surface after adding 60 mM fructose.
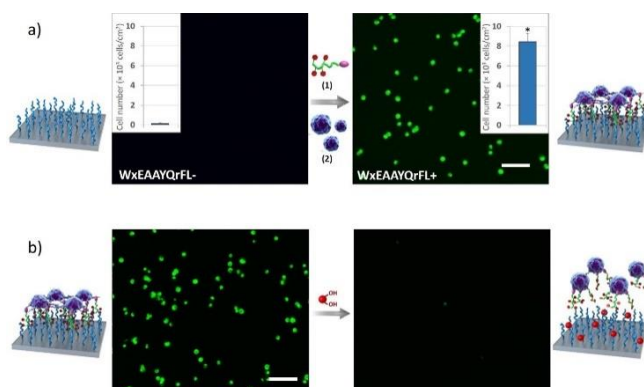

Figure 3. cancer cell capture and release on the sugar-responsive biointerface. a) MCF-7 cells (green, stained with DiO) can be efficiently captured onto the (DOPA)$_4$-S$_5$-WxEAAYQrFL-bound surface in 1 hour. b) The bound MCF-7 cells could be efficiently released (0.5 hour) by adding 60 mM fructose in the medium. Scale bar is 100 μm.

To further investigate the cell selectivity of our system, we set up a cell-capture experiment using a mixture (1:1) of green fluorescently stained MCF-7 cells and red stained HL60 cells (non-targeted human promyelocytic leukemia cells). After binding with (DOPA)$_4$-S$_5$-WxEAAYQrFL, the surface was then incubated into medium with the cell mixture to demonstrate the ability to recognize and isolate targeted MCF-7 cells. After incubation at 37 °C for 60 min, the MCF-7 cells were selectively captured onto the surface and almost no HL60 cells could be captured (Figure 4). Quantitative studies revealed that the proportion of MCF-7 cells among the captured cells was as high as 98.1 ± 0.7%. This result confirmed the ability of our dynamic biointerface to selectively recognize and capture targeted

cancer cells. Moreover, we can imagine that the flexibility of using mussel-inspired peptides with different cell-targeting sequences will endow the dynamic biointerface with desired cell selectivity.
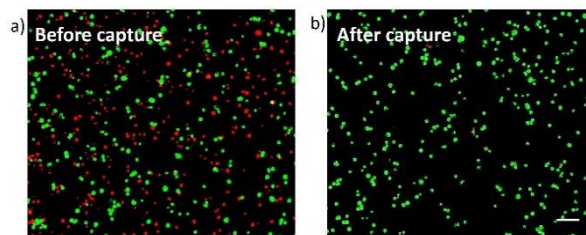

Figure 4. The selectivity of cancer cell capture on the dynamic biointerface. a) The representative fluorescent images of a mixed cell suspension containing 1:1 MCF-7 cells (green, DiO) and HL60 cells (red, DiI). b) The surface with (DOPA)$_4$-S$_5$-WxEAAYQrFLcould selectively capture MCF-7 cells from the mixed cell suspension. Scale bar is 100 μm.

In summary, we have developed a mussel-inspired dynamic biointerface based on reversible catechol-boronate chemistry. Dynamic presentation of cell-binding motifs at the interface can be easily achieved through sugar-responsive catechol-boronate interactions between biomimetic peptides and PBA polymer-grafted substrates. Moreover, by rational design of mussel-inspired peptides capped with different cell-binding sequences, the biointerface enables not only dynamic modulation of stem cell adhesion behaviors, but also selective isolation of tumor cells. Therefore, our mussel-inspired dynamic biointerface holds great promise in areas ranging from fundamental cell biology research to cell-based medical applications.

Acknowledgements

[1] a) N. Huebsch, D. J. Mooney, *Nature* **2009**, *462*, 426; b) W. P. Daley, S. B. Peters, M. Larsen, *J. Cell Sci.* **2008**, *121*, 255-264; c) J. Robertus, W. R. Browne, B. L. Feringa, *Chem. Soc. Rev.* **2010**, *39*, 354-378.
[2] K. S. Midwood, L. V. Williams, J. E. Schwarzbauer, *Int. J. Biochem. Cell B.* **2004**, *36*, 1031-1037.
[3] I. J. Fidler, *Nat. Rev. Cancer* **2003**, *3*, 453.
[4] a) P. M. Mendes, *Chem. Soc. Rev.* **2008**, *37*, 2512-2529; b) A. M. Rosales, K. S. Anseth, *Nat. Rev. Mater.* **2016**, *1*, 15012.
[5] a) H. Liu, X. Liu, J. Meng, P. Zhang, G. Yang, B. Su, K. Sun, L. Chen, D. Han, S. Wang, *Adv. Mater.* **2013**, *25*, 922-927; b) G. Pan, Q. Guo, Y. Ma, H. Yang, B. Li, *Angew. Chem. Int. Ed.* **2013**, *52*, 6907-6911; c) E. Wischerhoff, K. Uhlig, A. Lankenau, H. G. Börner, A. Laschewsky, C. Duschl, J. F. Lutz, *Angew. Chem. Int. Ed.* **2008**, *47*, 5666-5668.
[6] W. Li, J. Wang, J. Ren, X. Qu, *Angew. Chem. Int. Ed.* **2013**, *52*, 6726-6730.
[7] a) A. Pranzetti, S. Mieszkin, P. Iqbal, F. J. Rawson, M. E. Callow, J. A. Callow, P. Koelsch, J. A. Preece, P. M. Mendes, *Adv. Mater.* **2013**, *25*, 2181-2185; b) C. L. Yeung, P. Iqbal, M. Allan, M. Lashkor, J. A. Preece, P. M. Mendes, *Adv. Funct. Mater.* **2010**, *20*, 2657-2663; c) C. C. A. Ng, A. Magenau, S. H. Ngalim, S. Ciampi, M. Chockalingham, J. B. Harper, K. Gaus, J. J. Gooding, *Angew. Chem. Int. Ed.* **2012**, *51*, 7706-7710; e) Q. An, J. Brinkmann, J. Huskens, S. Krabbenborg, J. de Boer, P. Jonkheijm, *Angew. Chem.* **2012**, *124*, 12399-12403.
[8] a) J. Boekhoven, C. M. Rubert Pérez, S. Sur, A. Worthy, S. I. Stupp, *Angew. Chem. Int. Ed.* **2013**, *52*, 12077-12080; b) Z. Zhang, N. Chen, S. Li, M. R. Battig, Y. Wang, *J. Am. Chem. Soc* **2012**, *134*, 15716-15719; c) G. Pan, B. Guo, Y. Ma, W. Cui, F. He, B. Li, H. Yang, K. J. Shea, *J. Am. Chem. Soc* **2014**, *136*, 6203-6206; d) G. Pan, S. Shinde, S. Y. Yeung, M. Jakštaitė, Q. Li, A. G. Wingren, B. Sellergren, *Angew. Chem. Int. Ed.* **2017**, *56*, 15959-15963; e C. Zhao, I. Witte, G. Wittstock, *Angew. Chem. Int. Ed.* **2006**, *45*, 5469-5471. f) X. Qu, S. Wang, Z. Ge, J. Wang, G. Yao, J. Li, X. Zuo, J. Shi, S. Song, L. Wang, *J. Am. Chem. Soc* **2017**, *139*, 10176-10179.
[9] a) H. Zhang, D. Wang, X. Lin, N. Politakos, J. S. Tuninetti, S. E. Moya, C. Gao, *Sci. China Chem.* **2018**, *61*, 54-63; b) P. Shi, E. Ju, Z. Yan, N. Gao, J. Wang, J. Hou, Y. Zhang, J. Ren, X. Qu, *Nat. Commun.* **2016**, *7*, 13088; c) J. Auernheimer, C. Dahmen, U. Hersel, A. Bausch, H. Kessler, *J. Am. Chem. Soc* **2005**, *127*, 16107-16110; d) T. Wei, W. Zhan, Q. Yu, H. Chen, *ACS Appl. Mater. Inter.* **2017**, *9*, 25767-25774; f) D. Liu, Y. Xie, H. Shao, X. Jiang, *Angew. Chem. Int. Ed.* **2009**, *48*, 4406-4408; g) W. Li, Z. Chen, L. Zhou, Z. Li, J. Ren, X. Qu, *J. Am. Chem. Soc* **2015**, *137*, 8199-8205; h) S.-W. Lv, Y. Liu, M. Xie, J. Wang, X.-W. Yan, Z. Li, W.-G. Dong, W.-H. Huang, *ACS Nano* **2016**, *10*, 6201-6210; j) L. F. Kadem, M. Holz, K. G. Suana, Q. Li, C. Lamprecht, R. Herges, C. Selhuber-Unkel, *Adv. Mater.* **2016**, *28*, 1799-1802; k) P. Shi, E. Ju, J. Wang, Z. Yan, J. Ren, X. Qu, *Mater. Today* **2017**, *20*, 16-21.
[10] K. Uto, J. H. Tsui, C. A. DeForest, D.-H. Kim, *Prog. Polym. Sci.* **2017**, *65*, 53-82.
[11] a) H. Lee, B. P. Lee, P. B. Messersmith, *Nature* **2007**, *448*, 338; b) A. R. Narkar, B. Barker, M. Clisch, J. Jiang, B. P. Lee, *Chem. Mater.* **2016**, *28*, 5432-5439; c) G. Pan, S. Sun, W. Zhang, R. Zhao, W. Cui, F. He, L. Huang, S.-H. Lee, K. J. Shea, Q. Shi, *J. Am. Chem. Soc* **2016**, *138*, 15078-15086.
[12] a) J. Su, F. Chen, V. L. Cryns, P. B. Messersmith, *J. Am. Chem. Soc* **2011**, *133*, 11850-11853; b) B. Guo, G. Pan, Q. Guo, C. Zhu, W. Cui, B. Li, H. Yang, *Chem. Commun.* **2015**, *51*, 644-647.
[13] a) P. K. Forooshani, B. P. Lee, *J. Polym. Sci. Pol. Chem.* **2017**, *55*, 9-33; b) Q. Wei, K. Achazi, H. Liebe, A. Schulz, P. L. M. Noeske, I. Grunwald, R. Haag, *Angew. Chem. Int. Ed.* **2014**, *53*, 11650-11655.

[14] Y. Li, W. Xiao, K. Xiao, L. Berti, J. Luo, H. P. Tseng, G. Fung, K. S. Lam, *Angew. Chem.* **2012**, *124*, 2918-2923.

[15] R. H. Unger, A. D. Cherrington, *J. Clin. Invest.* **2012**, *122*, 4-12.

[16] M. Voinova, M. Jonson, B. Kasemo, *Biosens. Bioelectron.* **2002**, *17*, 835-841.

[17] J. Yan, G. Springsteen, S. Deeter, B. Wang, *Tetrahedron* **2004**, *60*, 11205-11209.

[18] E. Ruoslahti, M. D. Pierschbacher, *Science* **1987**, *238*, 491-497.

[19] U. Hersel, C. Dahmen, H. Kessler, *Biomaterials* **2003**, *24*, 4385-4415.

[20] B. J. Green, T. Saberi Safaei, A. Mepham, M. Labib, R. M. Mohamadi, S. O. Kelley, *Angew. Chem. Int. Ed.* **2016**, *55*, 1252-1265.

[21] H. Etayash, K. Jiang, S. Azmi, T. Thundat, K. Kaur, *Sci. Rep.* **2015**, *5*, 13967.